Pure & Appl.Chem., Vol.54, No.7, pp.1297-1311, 1982.
Printed in Great Britain.

0033-4545/82/071297-15$03.00/0
Pergamon Press Ltd.
©1982 IUPAC

PRINCIPLES AND APPLICATIONS OF CHEMICAL VAPOR DEPOSITION (CVD)

Karl E. Spear

Materials Research Laboratory, Materials Science Department,
The Pennsylvania State University, University Park, PA 16802 USA

Abstract — Chemical vapor deposition (CVD) reactions are extremely important for preparing materials in today's modern technology, particularly for the preparation of thin films for electronic and optical devices, and high temperature hard coatings for applications requiring erosion and/or corrosion resistance. Developing a scientific understanding of these dynamic, steady state chemical reactions which involve gaseous and condensed phases requires modeling the processes by making use of the fundamental principles of chemistry, thermodynamics, chemical kinetics, mass transfer, and the flow behavior of gases. In this paper, the general characteristics and applications of CVD reactions are reviewed, and the chemical reactions for typical processes are given. The paper then focuses on our approach to developing the mechanistic logic for a general model for CVD which can be used to explain and predict the chemistry and rates of CVD processes

INTRODUCTION

A chemical vapor deposition (CVD) process is one in which a gaseous phase chemically reacts to produce one or more condensed phases (deposit) plus gaseous product species. A typical laboratory or industrial CVD process would involve a dynamic flow system in which gaseous reactants pass over a heated substrate. These gases react chemically to produce a condensed coating on the substrate plus product gases, and then these product gases plus any remaining reactant gases exit from the hot reaction zone.

A CVD process can be described in terms of the systems chemistry (chemical species, thermodynamics, kinetics, reaction mechanisms), mass transport (gaseous diffusion, forced convection), and gaseous flow behavior (types of flow, flow patterns, velocities). In keeping with the topic of this conference, The Chemistry of Materials at High Temperatures, we have focused on understanding and predicting the chemical behavior of CVD processes with the use of a model based on thermodynamic, kinetic, and mass transport principles.

Many of the ideas on vapor transport and gas-solid interactions which are used in the model have been published previously by Faktor and Garrett (1), Battat et al. (2), Shaw (3), Jones and Shaw (4), van den Brekel (5), Bloem (6), Rosenblatt (7,8), Schäfer (9), Spear (10), Alcock and Jeffes (11), and Wallace and Bowman (12), to mention only a few of the general publications used in the preparation of this article.

In this paper, we attempt to link and extend many of the previously published ideas into a more complete model for describing CVD systems. We have purposely kept the mathematical treatment simple so that the physical descriptions of the mechanistic steps being treated, and the chemical logic behind the linkages between these steps are not lost. Our reasoning has been that if the physical models of the mechanistic steps are sound, and if the linking of these steps is logical in terms of describing the overall CVD process, then the model will be basically sound, and the later inclusion of more detailed mathematical descriptions of the individual processes making up the model will be relatively easy.

However, before a discussion of the modeling of CVD systems is undertaken, a variety of technological applications are noted and examples of materials prepared by CVD are illustrated.

APPLICATIONS AND EXAMPLES

Soot on the bottom of cooking vessels heated over open fires was probably the first observed result of a CVD process. The discovery of hematite (Fe_2O_3) single crystals in the throats of old volcanoes provided evidence for the very early occurrence of vapor transport reactions (9). The hypothesized CVD reaction resulting in the formation of the crystals is:

$$2FeCl_3(g) + 3H_2O(g) = Fe_2O_3(s) + 6\ HCl(g)$$

The gaseous reactants in this case were most likely produced at hotter temperatures in the volcanoes by the occurrence of the reverse of the "CVD reaction" which produced the crystals. Processes such as this in which a condensed material is transported from one region to another in a system by the reversal of one chemical reaction are usually called "chemical transport reactions" (9).

The purification of many metals has been achieved by chemical transport reactions (9,13,14). The deposition steps for a few of these transport reactions are:

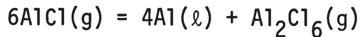

$$6AlCl(g) = 4Al(\ell) + Al_2Cl_6(g)$$

$$Ni(CO)_4(g) = Ni(s) + 4CO(g)$$

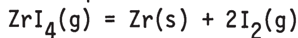

$$ZrI_4(g) = Zr(s) + 2I_2(g)$$

"Iodine lamps" are based on a chemical transport reaction involving reactions of tungsten metal with oxygen and iodine (15):

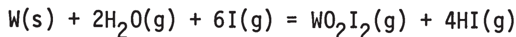

$$W(s) + 2H_2O(g) + 6I(g) = WO_2I_2(g) + 4HI(g)$$

The reaction proceeds from left to right at cooler filament temperatures to produce gaseous tungsten oxyiodides, and then proceeds from right to left at hotter temperatures (thin spots in the filament) to deposit tungsten and "heal" the thin portions of the filament.

The growth of large single crystals of ZnO(s) was achieved by Fischer (16) using a modified type of CVD process. The crystals produced in one experimental run are shown in Fig. 1.

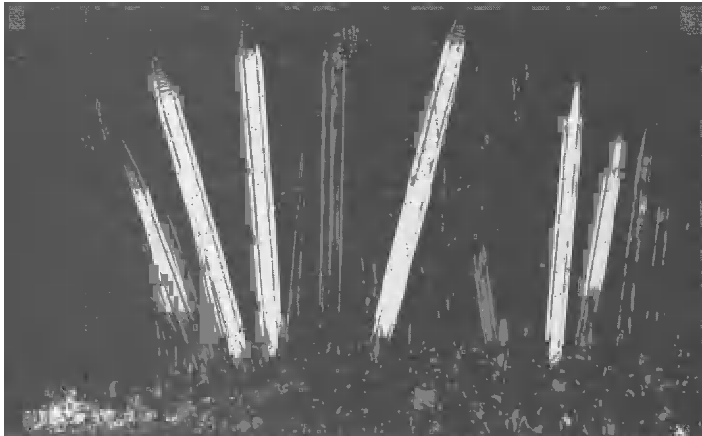

FIG. 1. Single Crystals of ZnO up to 6 cm in Length (Ref. 16).

They were nucleated and then grew out radially from a thin rod substrate. The net reaction producing the crystals was:

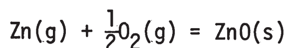

$$Zn(g) + \frac{1}{2}O_2(g) = ZnO(s)$$

The zinc vapor and either air or pure oxygen entered the reaction zone from opposite sides of the system so that the highest degree of supersaturation occurred in the region of the substrate rod. The zinc reactant gas was produced by the chemical reaction:

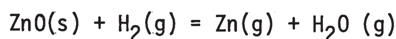

$$ZnO(s) + H_2(g) = Zn(g) + H_2O\ (g)$$

This process, just like the above chemical transport reaction processes, is not a "typical" CVD process, but the modeling principles discussed in this paper for CVD reactions can be applied to all of the above reactions.

The primary applications of CVD processes today center around the production of thin films for semiconductors and other solid state electronic and optical devices, coatings for cutting tools and other surfaces needing erosion and/or corrosion protection, coatings on fibers used in forming composite materials, and containment coatings for nuclear fuel and nuclear waste particles. CVD processes are also used in forming complex parts out of materials such as tungsten, molybdenum, rhenium, and high temperature, hard materials which resist conventional

machining and fabrication techniques.

Many examples of CVD research related to all of the above areas are found in the proceedings of the eight international conferences devoted to CVD (17-24). A few examples are briefly discussed below, but the reader should refer to the eight conference proceedings and the references cited therein for more detail.

Important materials being prepared by CVD for electronic and optical devices include Si, Ge, Si_3N_4, SiO_2, GaAs, CdS, ZnSe, and related compounds. Bloem (6) has recently summarized research on the CVD of silicon for semiconductor technology. The overall CVD reactions receiving the most attention are:

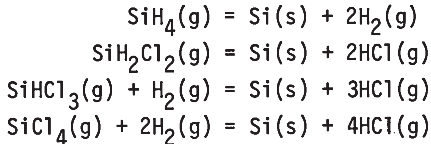

$$SiH_4(g) = Si(s) + 2H_2(g)$$
$$SiH_2Cl_2(g) = Si(s) + 2HCl(g)$$
$$SiHCl_3(g) + H_2(g) = Si(s) + 3HCl(g)$$
$$SiCl_4(g) + 2H_2(g) = Si(s) + 4HCl(g)$$

Most of the studies have been carried out in flowing, one atmosphere systems which use a hydrogen carrier gas with approximately one percent or less silicon containing species. Since the solid deposit (Si) is chemically quite simple, most research efforts have focused on nucleation, chemical kinetics, mass transport, and gas flow behavior of the systems. Purity, crystalline perfection, and uniformity of deposit thickness over the substrate wafers are parameters of importance in such studies. A number of modeling studies have been carried out on these systems, and have been referenced by Bloem (6).

Erosion and corrosion resistant coatings commonly applied by CVD to tooling materials are titanium carbide, titanium nitride, chromium carbide, and aluminum oxide (25). In addition, an appreciable amount of CVD research is being performed on coatings of TaC, TaN, W_2C, TiB_2, SiC, Si_3N_4, B_4C and B for use on cutting tools, fibers, and applications in which the materials are subjected to high temperature, corrosive and erosive environments. Fig. 2 shows a

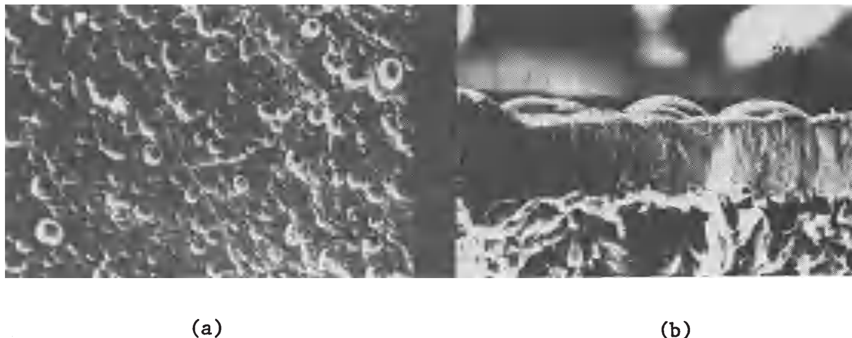

(a) (b)

FIG. 2. Surface (a) and Cross Section (b) of CVD TiB_2 Coating on Graphite (Ref. 26).

coating of TiB_2 on graphite which was deposited at 900°C as part of a fundamental study of the CVD of TiB_2 (26-28). Fig. 3 shows the results when bundles of carbon fibers which made up carbon cloth were subjected to the CVD of TiB_2 at different temperatures (29). Only at the lower temperatures would the deposits penetrate into the center of the bundles. The net CVD reaction used in both of these studies was:

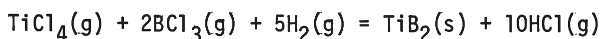

$$TiCl_4(g) + 2BCl_3(g) + 5H_2(g) = TiB_2(s) + 10HCl(g)$$

Fig. 4(a) shows a cross section of a 1/2" O.D. tungsten tube with its inside walls coated (30), Fig. 4(b) shows a cross section of a carbon fiber which has been coated with NbC_xN_y (31) by a CVD process. Fig. 5 shows the striated surface of an uncoated tungsten filament, and a boron coated filament which shows the preferential nucleation of boron on the ridges of the filament (32).

The cross section of a gas cooled reactor nuclear fuel particle made by the fluidized bed coatings a microsphere of UO_2 is shown in Fig. 6 (33). The first of four coatings is a

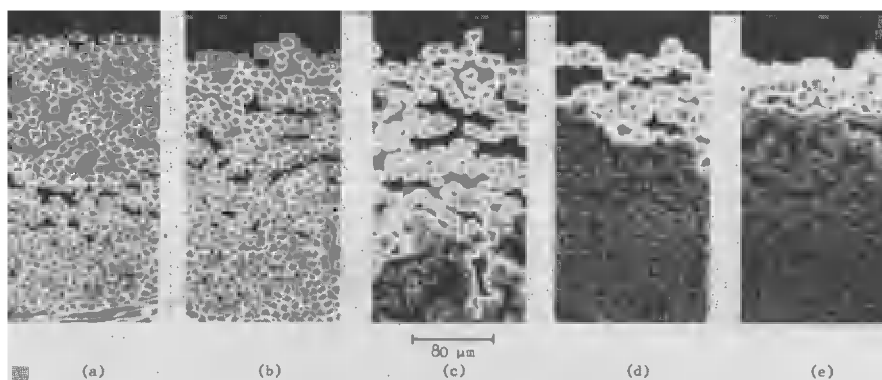

FIG. 3. Titanium Diboride Coated Carbon Cloth as Deposited at (a) 700°C, (b) 750°C, (c) 800°C, (d) 900°C, and (e) 1000°C. Shown are the cross sections of bundles of fibers which make up a strand of the cloth (Ref. 29).

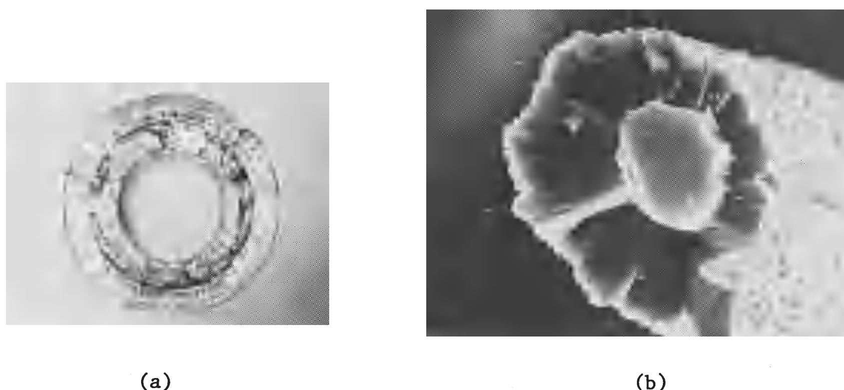

(a) (b)

FIG. 4. (a) Tungsten Tube Cross Section with B_4C Coating on Inside Walls (Ref. 30). (b) Carbon Fiber Coated with NbC_xN_y (Ref. 31).

porous carbon "buffer layer," the second one a dense pyrolytic graphite layer, the third a silicon carbide layer, and the fourth another pyrolytic graphite layer. The porous layer is typically obtained by pyrolyzing acetylene, while the two dense graphite layers are obtained by pyrolyzing a hydrocarbon such as propene. The net reaction used to obtain the silicon carbide coating is:

$$CH_3SiCl_3(g) = SiC(s) + 3HCl(g)$$

Another nuclear application of fluidized bed coating technology is the coating of nuclear waste particles with various materials in attempts to isolate and contain the radioactive elements (34).

Most of the above systems are chemically more complex than those used in the CVD of silicon; more gaseous species are possible, several solid phases may deposit, and some of the solid phases exhibit solid solution ranges. Attempts to develop a scientific understanding of these chemically complex systems has become more common in recent years, as the CVD Conference Proceedings mentioned above clearly illustrate. Vandenbulcke (35) just recently included the homogeneity range of TiC in his thermodynamic analysis of the CVD conditions needed to deposit this phase. Besmann and Spear (26-28) have correlated their experimental results on the CVD of TiB_2 with thermodynamic and kinetic models for the process. Spear (10) and

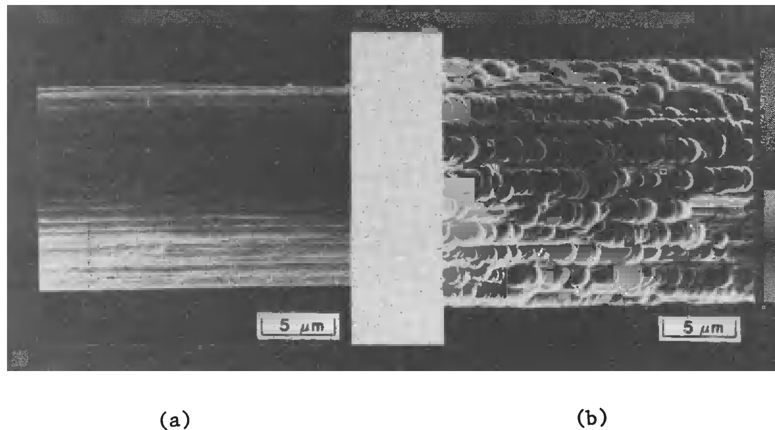

(a) (b)

FIG. 5. (a) Tungsten Filament, and (b) Boron Coated Filament (Ref. 32).

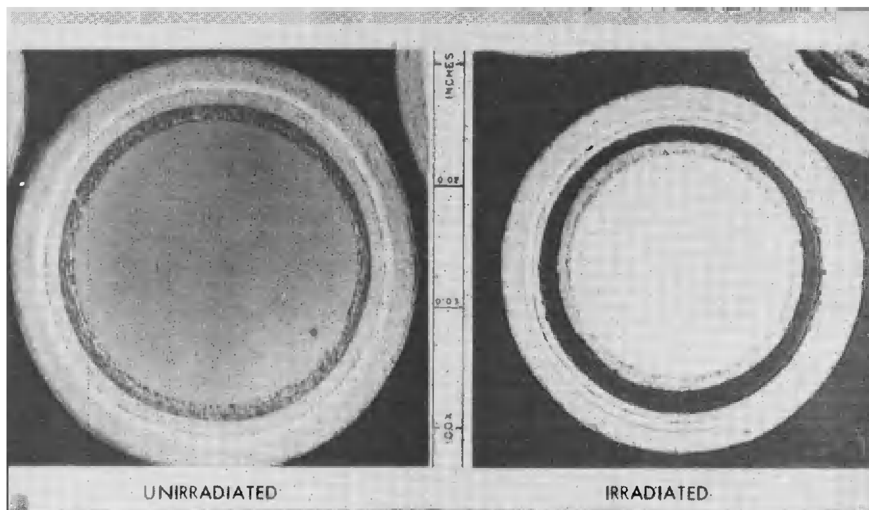

FIG. 6. Unirradiated and Irradiated TRISO Coated Nuclear Fuel Particle for a Gas Cooled Reactor (Ref. 33).

Bernard (36) have both reviewed applications of thermodynamic and phase equilibria principles to CVD processes.

Most of the research on the CVD of a refractory metal has been concerned with tungsten. As Blocher (37) points out in a review of structure-property-process relationships in CVD, forty-two papers on the CVD of tungsten appeared in the first four CVD conference proceedings (17-20). The overall reaction typically used to deposit tungsten is:

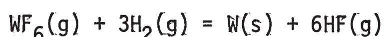

$$WF_6(g) + 3H_2(g) = W(s) + 6HF(g)$$

The fabrication of containers, heat shields, and other pieces of equipment and devices which need to exhibit mechanical integrity and strength. Therefore, the relationship of the process parameters to the physical structure of the deposits has been of primary concern. The nature of these studies has been similar to those on the CVD of silicon in that both systems have relatively simple chemistry in comparison with those involved in the deposition of some of the above high temperature, refractory coatings.

MODELING CVD PROCESSES

We are attempting to develop a model which will describe the behavior of a dynamic chemical system in which a reactive gas flows over a heated substrate. For modeling the chemistry of the system, we make use of thermodynamic calculations where localized equilibrium exists, accepted equations for describing adsorption and desorption, and standard chemical kinetic

reaction equations. The mass transfer is described by forced convection, Fick's first law, and Stefan flow equations.

We have adopted a simple, but useful boundary layer model for the gas flow over a solid substrate, always remembering that we ultimately wish to couple our detailed model describing the chemical and mass transport processes occurring with a more exact model describing the gas flow. A detailed description of the gas flow behavior at each point in a system is extremely important, especially when uniform deposits are sought, but this is a specialized area of research which will not be discussed here.

A primary concern throughout out attempts to develop a predictive mathematical model for describing the chemical behavior of CVD has been to provide a schematic physical model of the system and of each step in the process. These physical pictures have provided insight into the processes, and have helped both in understanding observed behavior and in designing meaningful experiments. They have also enhanced our development of the logic behind the calculations based on the model.

Assumptions and Boundary Conditions

Fig. 7 schematically illustrates the assumed experimental system to be modeled. Only isothermal, isobaric conditions are considered for the present discussion, although the non-isothermal conditions typical of a cold-walled reactor could be readily incorporated into the model.

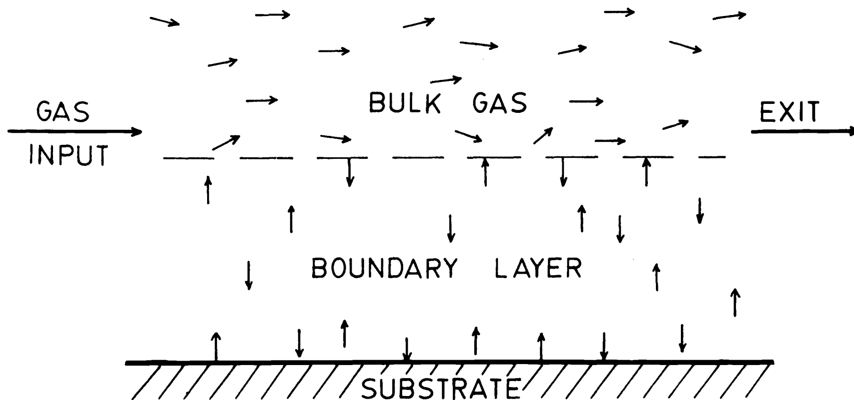

FIG. 7. Boundary Layer Model for the Gas in a Flowing CVD System.

Complete mixing to form a homogeneous gas is assumed in the bulk gas region, while the gas in the boundary layer region adjacent to the substrate is assumed to mix only by gaseous diffusion between the substrate and the bulk gas. The gaseous boundary layer, whose thickness is determined by the gas flow behavior of the system, can thus develop partial pressure gradients between the substrate and the bulk gas region. Within any given volume element of the system being analyzed, partial pressure gradients parallel to the substrate are not allowed. The model thus restricts diffusive mass transport to directions perpendicular to the substrate.

Another important assumption in our model is that steady state conditions exist. In other words, the properties at any particular location in the system are constant, independent of time. The steady state conditions place critical restrictions on the material flux through the system.

We have also assumed that no chemical reactions occur among the gases in the bulk gas or boundary layer regions, but that all chemical reactions occur at the substrate.

In addition to the imposed boundary conditions of constant temperature and constant total pressure for the system, two additional boundary conditions exist. The first is conservation of mass. The rate of input of each element into the system must equal the exit rate plus the deposition rate for the element.

The other boundary condition is a consequence of the steady state conditions assumed for the system. As is discussed in some detail in the next section, the overall CVD process is modeled by sequential connections of "links," with each sequential link being composed of an individual process, or of two or more processes occurring in parallel. Examples of individual

processes are diffusion through a boundary layer, adsorption, etc. The boundary condition imposed by the steady state assumption is that the rate of flow of a given element through a link must be identical for all links unless the element is removed by the deposition process. Specific examples of modeling CVD systems which are given later in the paper will help to clarify and illustrate this important boundary condition.

The chemistry of the system also imposes restrictions in that the stoichiometry of each molecular species fixes the ratios of the elements for the processes in which the species is participating.

Uncoupling CVD Processes and the Equations for Uncoupled Steps

A net CVD process can be described by a series of mechanistic steps which can be coupled through mass and flux balances. The coupling is sequential with connections of "links." Each link in the sequence is either a unique mechanistic step, or two or more steps competing in parallel (1). Within the limitations of the boundary conditions discussed in the previous section, the link with the slowest maximum possible rate limits the overall rate for the process. Examples given later will help to clarify the analysis of CVD systems through the coupling of the individual mechanistic steps which can occur during the process.

A number of authors, including Shaw (3,4) and Faktor et al. (1,2), have listed and discussed the mechanistic steps which can occur during a vapor deposition process. Fig. 8 schematically shows the seven steps listed below:

1. Forced flow of reactant gases into the system.
2. Diffusion and Stefan flow of reactant gases through the gaseous boundary layer to the substrate.
3. Adsorption of gases onto the substrate.
4. Chemical reactions of the adsorbed species, or of adsorbed and gaseous species.
5. Desorption of adsorbed species from the substrate.
6. Diffusion and Stefan flow of product gases through the boundary layer to the bulk gas.
7. Forced exit of gases from the system.

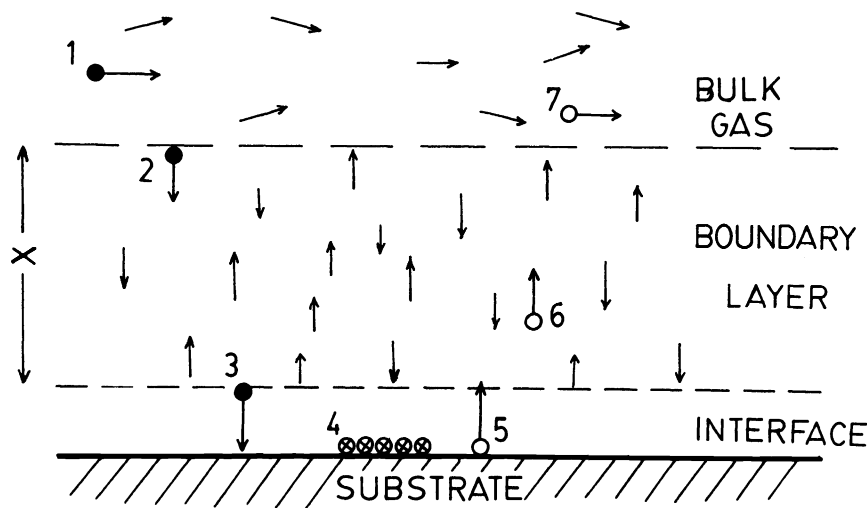

FIG. 8. Schematic Diagram Showing Seven Mechanistic Steps Which Occur During a CVD Process.

Steps 1 and 7 are mass transport steps, with the rate of step 1 determined completely by the experimentally controlled input gas flow rates. Step 7 is controlled by the system's total gas flow rate, with the chemistry of the gas determined by the nature and extent of the chemical reactions occurring in the system.

Steps 2 and 6 are mass transport processes through the boundary layer with rates which depend upon Fick's first law and Stefan flow equations. The corresponding flux equation for the mass transport of species (i) can be written as (1):

$$Ji = (U/RT)\cdot pi - (Dij/RT)\cdot(\partial pi/\partial x) \quad (1)$$

The first term on the right side of the equation gives the flux from Stefan flow, and the second term gives the flux from molecular diffusion. The symbols in the equation are defined as follows:

Ji = flux of species i through the boundary layer.
U = gas flow velocity perpendicular to the substrate caused by the change in the number of moles of gas during the chemical reactions occurring at the surface.
R = ideal gas constant.
T = absolute temperature.
pi = partial pressure of species i.
Dij = binary diffusion coefficient of species i through the carrier gas j. (For simplicity, we are assuming carrier gas j has a large partial pressure in comparison with the other gaseous species).
$\partial pi/\partial x$ = the partial pressure gradient of species i perpendicular to the substrate.

As has been illustrated previously (28), Dij and ∂x can be expressed as functions of temperature, pressure, and flow rates.

Steps 3, 4, and 5 can be activated chemical processes with rate constants which follow an Arrhenius relationship. Steps 3 and 5 are not likely to be important rate limiting steps unless the species are chemisorbed with activation energies similar to condensation energies. The flux of species (i), JAi, which strike the surface and are adsorbed (not reflected back into the gas phase) is given by the equation:

$$JAi = \delta \cdot pSi/(2\pi M_i RT)^{1/2} \quad (2)$$

while the flux of species (i), JDi, desorbed from the surface is given by a similar equation:

$$JDi = \delta \cdot pEi/(2\pi M_i RT)^{1/2} \quad (3)$$

The term δ is the fraction of the total species striking the surface which actually adsorb, and is also equal to the fraction of species which actually desorb as compared to the number which would desorb if no kinetic barriers to the desorption process existed (8).

The pSi term is the gas partial pressure of species (i) at the surface just above the substrate. The term pEi is the gas partial pressure of species (i) which would be in equilibrium with the concentration of adsorbed species (i) which exists on the surface. In other words, the gas with pressure pEi has the same chemical potential as the adsorbed species on the surface.

The net flux of adsorbing species (i), JNi, is just:

$$JNi = JAi - JDi \quad (4)$$

or,

$$JNi = \delta \cdot (pSi - pEi)/(2\pi M_i RT)^{1/2} \quad (5)$$

For reactant species, where JNi is positive since there is a net flux of molecules to the surface where the deposition process is occurring, the value of pSi may approach pEi, but it must always be slightly larger. The opposite is true of product species, where JNi is negative since there is always a net flux of molecules away from the surface. Then pSi may approach pEi, but it must always be slightly smaller.

Step 4 may mechanistically consist of several chemical reactions on the surface which combine to give the overall net deposition reaction. Typically, we do not know the detailed mechanisms of the surface processes, but we can represent the rate of the net reaction by an equation:

$$R(deposit) = K \cdot f(pEi) \quad (6)$$

where R(deposit) is the rate of formation of the deposited phase, K is a rate constant which follows an Arrhenius equation of the form:

$$K = K_0 \cdot \exp(E/kT) \quad (7)$$

K_0 is a constant, and E is the activation energy for the process. The term f(pEi) represents some function of the equilibrium partial pressures of the adsorbed species. As mentioned above, the pressures represented by pEi are those which would be in equilibrium with the existing concentration of adsorbed species on the surface, and are thus a measure of the chemical potentials of those species.

Coupling CVD Processes and the Implications of Various Rate Limiting Steps

The analysis of a specific CVD process involves determining the experimental dependence of deposition behavior with changes in controllable experimental variables, and then correlating these results with those implied by various possible mechanisms which could limit the overall rate of the process.

For example, if the deposition rate depends strongly upon the input gas flow rates, then thermodynamic limits for the process are almost certainly the most important factor limiting the deposition rate in the process.

If the deposition rate is relatively independent of input gas flow rates, then either the mass transport rate of gas in or out of the gaseous boundary layer, or the rate of a chemical kinetic rate limiting mechanism at the substrate (adsorption, desorption, or a surface reaction) must be limiting the overall rate of the deposition process. The temperature dependence of the deposition rate will usually differentiate between gaseous diffusion limiting steps (weak dependence) and surface reaction limiting steps (strong dependence). However, as is illustrated in the discussions below, the coupling of the various possible rate limiting mechanisms provides a more complete analysis.

(a) Rate Limiting Step of the Input Gas Flow Rates. If the residence time of the reactant gases in the reaction zone of the system is long in comparison with gaseous diffusion rates and the rates of chemical reactions, then the thermodynamic properties of the system will ultimately limit the deposition rate for the process.

In this discussion, we will consider only the simplest case in which a gas enters a reaction zone, resides there until all chemical processes reach equilibrium, and then the equilibrium gas phase exits out of the system as new gas enters. Schematic plots of the relative partial pressures of reactant and product gases as a function of distance away from the substrate are shown in Fig. 9. Since all the gases are in equilibrium, no gradients in partial pressure (or chemical potential) exist across the boundary layer between the bulk gas and the substrate, or between the gas and the adsorbed species at the substrate-gas interface.

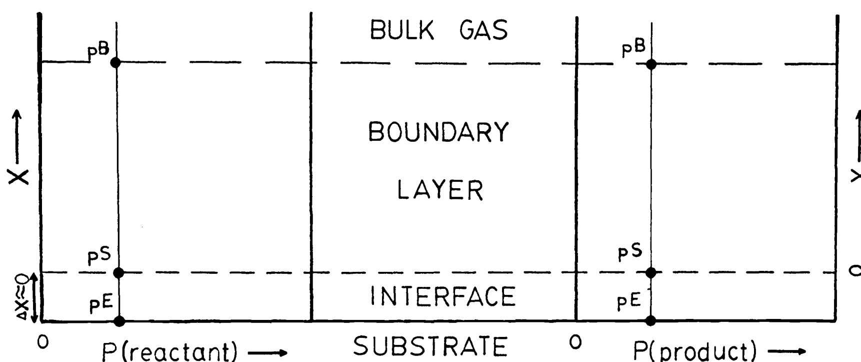

FIG. 9. Schematic Plots of Relative Partial Pressures of a Reactant Gas and a Product Gas as a Function of Distance from the Substrate for a CVD Process Limited by the Input Gas Flow Rates.

For this limiting case, equilibrium calculations can accurately predict which phases can deposit, their rates and efficiencies of deposition, and the partial pressures of all possible gaseous species. The predictions can be made as a function of the experimental variables of temperature, total pressure, and the composition and total flow rate of the input gas phase. These predictive calculations have been reviewed in detail previously (10,36).

Examples of two "CVD phase diagrams," a term coined for diagrams depicting which solid phases would deposit as a function of experimental variables (27), are given in Fig. 10 for low pressure CVD (LPCVD) systems used for producing Si_3N_4 and SiO_2 films in the electronics industry (38). Input gases are SiH_2Cl_2 and NH_3 for producing Si_3N_4, and SiH_2Cl_2 and N_2O for producing SiO_2. The solid phases which can deposit under the experimental conditions shown are depicted by these diagrams. At higher temperatures in the SiH_2Cl_2-N_2O system, and a ratio of input gases on the order of unity, no solid phase will deposit at equilibrium. As the diagrams show, several regions of experimental conditions exist under which two or three solid phases can exist together with the gas at equilibrium.

(b) Rate Limiting Step of Mass Transport Through a Boundary Layer. If the input gas rates and the rates of chemical reactions are rapid in comparison with gaseous diffusion, then the rate limiting step for a CVD process will be the mass transport of material through the gaseous boundary layer above the substrate.

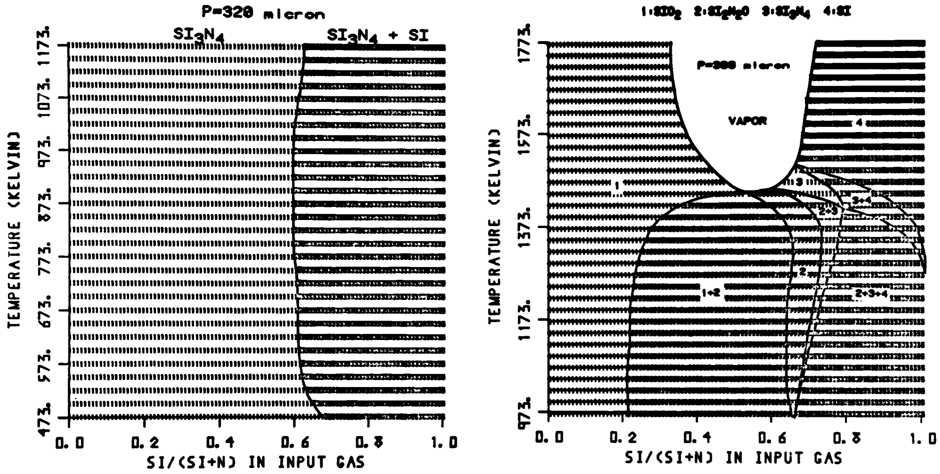

FIG. 10. CVD Phase Diagrams for LPCVD Systems with Reactant Gases of (a) SiH_2Cl_2-NH_3, and (b) SiH_2Cl_2-N_2O (Ref. 38).

Schematic plots of the relative partial pressures of reactant and product gases as a function of the distance above the substrate are shown in Fig. 11 for a steady state CVD process limited by mass transport through a gaseous boundary layer. This diagram, and the discussion which follows, considers only the initial reaction processes when the bulk gas contains reactant gases with their initial input partial pressures, and no product gases. The gas and substrate are also assumed to be in equilibrium at their interface.

To illustrate the analysis and some of the consequences of a CVD process being limited by mass transport through a boundary layer, we will consider a simple reaction of the reduction of a metal halide MX_2 with hydrogen gas to deposit the metal on a substrate. We will assume

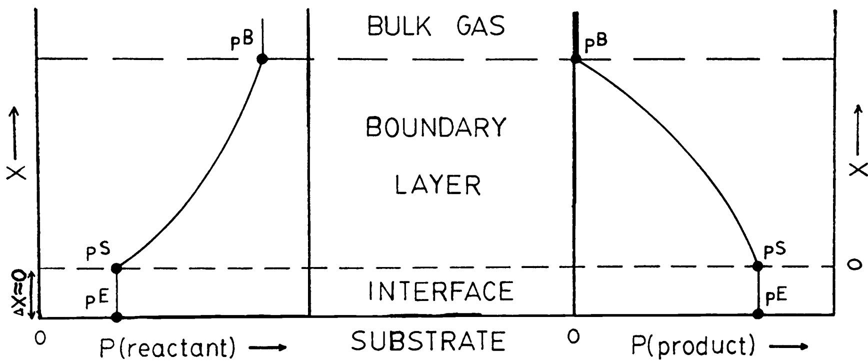

FIG. 11. Schematic Plots of Relative Partial Pressures of a Reactant Gas and a Product Gas as a Function of Distance from the Substrate for a Steady State CVD Process Limited by Mass Transport through a Boundary Layer.

the only reaction of importance is:

$$MX_2(g) + H_2(g) = M(s) + 2HX(g) \quad (8)$$

Since the number of moles of gaseous product is the same as the number of reactant gases, no Stefan flow occurs, and the flux equation for each gaseous species (i) as given by Eq. 1 can be simplified and integrated between the limits of the boundary layer to give:

$$J_i = -(D_i/xRT)\cdot(p^S_i - p^B_i) \quad (9)$$

where x is the boundary layer thickness, pSi is the partial pressure of (i) at the substrate, and pBi is the partial pressure of (i) in the bulk gas. This equation represents the flux from the bulk gas to the surface.

Since equilibrium is assumed at the interface between the surface and the gas, the pSi values can be replaced by pEi values, the pressures in equilibrium with the surface adsorbed species. Also, for the initial reaction process being considered, the pBi values for MX_2 and H_2 are the initial input partial pressures, represented by pINi, and the pBi value for HX is equal to zero. Thus, we can write the flux equations for the three gaseous species in the system as follows:

$$J(MX_2) = -(D1/xRT)\cdot(pE1 - pIN1); \quad 1 = MX_2 \tag{10}$$

$$J(H_2) = -(D2/xRT)\cdot(pE2 - pIN2); \quad 2 = H_2 \tag{11}$$

$$J(HX) = -(D3/xRT)\cdot(pE3 - 0); \quad 3 = HX \tag{12}$$

If we know the diffusion coefficients (Di) for each species, and we know the boundary layer thickness (x), then we are left with six unknown quantities, the three fluxes (Ji) and the three partial pressures in equilibrium with the surface (pEi). These can be calculated with the use of the above three flux equations and the three following independent equations.

The steady state assumption places requirements on the relative fluxes. Since the reaction represented by Eq. 8 is the only one of importance, the stoichiometry requires that:

$$J(MX_2) = J(H_2) \tag{13}$$

$$J(MX_2) = -\frac{1}{2} J(HX) \tag{14}$$

The negative sign is a result of the fact that all the fluxes represent the flow of material from the bulk gas to the surface. The requirement of a constant total pressure in the system provides another relationship between the partial pressures of the gases at the surface:

$$P(total) = pE1 + pE2 + pE3 \tag{15}$$

The above six equations (10-15) allow us to calculate the unique pressures of the gases in equilibrium with the surface. The gases with these partial pressures are assumed to be in equilibrium with the surface adsorbed species, but no assumptions were made about the deposition reaction (Eq. 8) being in equilibrium at the surface. In fact, satisfying the above steady state flux requirements and the constant total pressure requirement fixes the partial pressures at unique values which are independent of the equilibrium constant for the deposition reaction. However, as will become apparent from the discussions in the following paragraph concerning the approach of the system toward steady state conditions, the unique pEi pressures calculated from Eqs. 10-15 above may not always be achieved. In fact, satisfying Eqs. 10-15 may require one or more negative pEi values, which is physically unrealistic. If this occurs, the analysis must proceed as in the following discussion.

A more detailed examination of the relationships between the flux equations and requirements, and the equilibrium constant for the deposition reaction will help to clarify and to model the CVD processes occurring. We will do this by considering the approach of the previously discussed system toward the steady state conditions in which mass transport through a boundary layer is the slowest step in the process.

At the first point in time that the deposition reaction occurs, before any partial pressure gradients are developed, the partial pressures of the reactant gases at the surface are those of the input gas. We will consider the conditions in which we allow this reactant gas to react according to Eq. 8 and reach equilibrium. This equilibrium model places three restrictions on the system. First, as in the steady state situation, the total pressure of the system remains constant:

$$P(total) = pEQ1 + pEQ2 + pEQ3 \tag{16}$$

where 1, 2, and 3 are used as previously to denote MX_2, H_2, and HX, respectively. The pEQi symbol is used to designate the gas with this pressure is in complete equilibrium with the solid deposit and other gases (as well as the adsorbed species), while the pEi symbol designating the gas is in equilibrium with the adsorbed species on the surface.

A second restriction is a result of the equilibrium, through the relationship given by the equilibrium constant:

$$K(T) = pEQ3^2 / pEQ1\cdot pEQ2 \tag{17}$$

A third restriction is on the gas composition. The fraction n(X)/n(H), the concentration of X divided by the concentration of H in the gas, is fixed by the input gas composition since neither X nor H are removed from the gas phase by the deposition process. The resulting equations are:

$$n(X)/n(H) = pIN1/pIN2 \tag{18}$$

$$pIN1/pIN2 = (2\cdot pEQ1 + pEQ3)/(2\cdot pEQ2 + pEQ3) \tag{19}$$

We have the three unknowns of pEQ1, pEQ2, and pEQ3, and the three equations 16, 17, and 19 which will allow us to determine these three unique equilibrium pressures. If we substitute these equilibrium pressures for the pEi values in the flux equations given in 10, 11, and 12, we can calculate the relative fluxes for the three gaseous species just as the initial deposition begins. As the deposition reaction proceeds, the partial pressures at the surface will change from the pEQi values toward the pEi values, and the fluxes will change accordingly from those fixed by the initial equilibrium at the surface toward the values fixed by the steady state deposition conditions. Another way of saying this is that the partial pressures at the surface change from values which initially obeyed the conditions imposed by Eqs. 17 and 19 toward values which obey the steady state requirements represented by Eqs. 13 and 14.

It is informative to carry this discussion further by considering the implications of initial flux relationships on the systems approach toward steady state conditions. If $J(MX_2) < J(H_2)$ initially, then the pressure of H_2, pE2 will tend to build up at the surface, which will drive the deposition reaction to the right, causing the pressure of MX_2, pE1, to decrease at the surface. The increase in the hydrogen pressure and the decrease in the MX_2 pressure at the surface will occur until $J(MX_2) = J(H_2)$, the requirement for steady state conditions.

Another example to consider is when the initial flux relationship of $J(MX_2) < -1/2\ J(HX)$ exists. As the system moves toward the steady state conditions given in Eq. 14 of $J(MX_2) = -1/2\ J(HX)$, the pressure of HX would tend to decrease at the surface because of the initial flux relationship, which would drive the reaction (Eq. 8) further to the right to produce more HX and lower the pressure of MX_2 at the surface. The lowering of the MX_2 pressure will increase the flux of this species toward the surface up to a limiting maximum value which exists when $pE(MX_2) = 0$ at the surface. The above steady state relationship which is required between the fluxes of MX_2 and HX then allows us to calculate the limiting maximum value for J(HX), and thus the maximum value for the pressure pE(HX) at the surface.

The boundary condition of a constant total system pressure must also be taken into account when deducing how the system approaches steady state conditions. In the above example, for instance, it is very possible that the deduced limiting flux of MX_2 for $pE(MX_2) = 0$, and the corresponding limiting pE(HX) value calculated will with the $pE(H_2)$ partial pressure add up to give a total system pressure less than that specified for the system. Another way of saying this is that the attempt of the system to approach steady state conditions tends to decrease the total pressure of the system at the surface. Since this is impossible (no hinderances to flow exist perpendicular to the surface), a "net flow" of gas would occur from the bulk gas toward the surface in addition to the diffusional fluxes. This gas flow would increase the net flux of MX_2 toward the surface, and would decrease the net flux of HX away from the surface [-J(HX)]. Thus, this gas flow would speed up the approach to steady state conditions, and would increase the flux of MX_2 over its limiting diffusional value which exists when $pE(MX_2) = 0$. The corresponding deposition rate of M(s) would also be enhanced.

(c) Rate Limiting Step of Adsorption of a Reactant Gas Species. The present discussions of adsorption limitations on a CVD reaction will be directed only toward the logic of including an additional "link" in the CVD model. We will consider only steady state conditions, and use the example reaction discussed in the previous section of MX_2 gas being reduced by hydrogen to give M(s) and HX gas. We will assume that the adsorption of MX_2 gas onto the surface has a kinetic barrier, so that its surface pressure pS1 is greater than pE1, the pressure of MX_2 which would be in equilibrium with the actual concentration of adsorbed MX_2 species. Fig. 12 shows schematic plots of the partial pressures of MX_2, H_2, and HX as a function of distance from the substrate.

As in the mass transport limited case discussed in the previous section, the steady state conditions require the flux and pressure relationships given by Eqs. 10-15, except that for the adsorption limiting case, we will change the MX_2 pressure pE1 in Eqs. 10 and 15 to pS1 since the diffusional flux and system pressure depend on the surface pressures, not a pressure pE1 which is a measure of the chemical potential of the adsorbed surface species.

The relationships of Eqs. 10-15 allow us to determine values of pS1, pE2 (=pS2), and pE3 (=pS3), the respective pressures of MX_2, H_2, and HX at the surface. The actual diffusional fluxes of the three species can also be calculated from these equations. If we wish to know the value of pE1, the pressure of importance for driving the deposition reaction since it is a measure of the surface chemical potential of MX_2, then Eq. 5 which gives the net adsorption flux must be used:

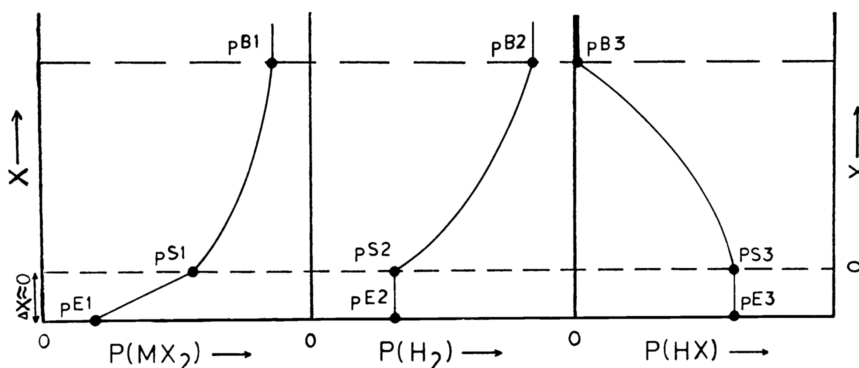

FIG. 12. Schematic Plots of the Relative Steady State Partial Pressures of MX_2, H_2, and HX as a Function of Distance from the Substrate When the Adsorption of MX_2 Exhibits a Kinetic Barrier.

$$JN1 = \delta \cdot (pS1 - pE1)/(2\pi M_1 RT)^{1/2} \tag{20}$$

and the value of δ the fraction of total species striking the surface which actually adsorb, must be known. Since the diffusional flux for MX_2 must equal the net adsorption flux, the value of pE1 is the only unknown to be calculated from Eq. 20.

The above mathematical procedure may yield pS1, pE2, and pE3 values which are non-negative, a requirement if the modeling is to be realistic, but Eq. 20 may then give a negative value for pE1 in order that the net adsorption flux of MX_2 be equal to that calculated for the diffusional flux of MX_2 to the surface. Since this is unrealistic, the value of pE1 should be set equal to zero for the flux equation (the value is obviously not zero since the chemical potential of the surface adsorbed species will not be zero, but it will be very small). In order for the diffusional and net adsorption fluxes to be equal, the surface pressure pS1 must be increased from the value calculated above using Eqs. 10-15 in order to decrease the diffusional flux and increase the adsorption flux of MX_2.

In addition, the decrease in the flux MX_2 must be accompanied by a decrease in the flux of H_2 and HX if steady state conditions are to exist. The decrease in the flux of H_2 can be achieved by increasing the pressure of this species at the surface, pE2. The decrease in the flux of HX can be achieved by decreasing the pressure of this species at the surface, pE3.

The net result of the above is that the surface partial pressures of the two reactants, MX_2 and H_2, increase, and the surface partial pressure of the product, HX, decreases. This change is not in conflict with maintaining a constant system pressure at the surface, but the change does tend to drive the deposition reaction to the right, toward the deposition of more material. An increase in the deposition will counteract the steady state changes by tending to decrease the partial pressures of MX_2 and H_2 and increase the partial pressure of HX. However, since the surface potential of MX_2 (as measured by its pE1 value) is very small, a lowering of the pE1 value can occur until the reaction on the surface is at equilibrium, and yet the changes in the fluxes will remain practically constant. For example, if pS1 is 0.2 atm, the change in pE1 from 10^{-4} to 10^{-8} atm will have a negligible effect on the net adsorption flux calculated from Eq. 20 above, but the change will have a great effect in terms of the activity quotient for the deposition reaction.

CONCLUDING REMARKS

It is apparent from the preceding sections that the development and applications of the discussed modeling techniques are in their infancy. Hopefully, it is also apparent that these techniques can provide a very descriptive and powerful method for analyzing the chemical and mass·transport reaction processes which occur in a CVD system.

The chemistry of the examples discussed in this paper was quite simple. Only the chemical species which participated in one chemical reaction were assumed to be important. However, the logic of the analysis procedure, and the boundary conditions for the process remain the same, even if a large number of gaseous species are present in significant quantities. The accounting may get complex in calculating the net flux for an element when it is present in

ten or more different species, but computers easily handle this type of problem. Our chief concern is making certain that the basic models for each mechanistic step in the CVD process are the best available, and that the coupling of the steps to describe the entire CVD process is logically correct.

If more than one solid phase can be deposited, then an equilibrium calculation involving the chemical potentials of the adsorbed species needs to be performed to determine which of the various condensed phases is thermodynamically stable. Otherwise, experimental information as to which condensed phase(s) forms can be fed back into the analysis. For chemically complex systems, assumptions as to local equilibrium will have to be made to determine, for example, concentrations of adsorbed gaseous species when a slow deposition reaction is limiting the rate of deposition.

Today's modern technology requires materials that will withstand higher temperatures and more corrosive and/or erosive environments. To meet these requirements, a knowledge of how to produce protective coatings with a high reliability is needed. Developing an understanding of the processes occurring in CVD systems will greatly enhance our abilities in this area, as well as for any heterogeneous chemical process occurring in a dynamic flow system. For example, the modeling techniques outlined in this paper for CVD systems are just as valid for the analysis of corrosion by a flowing gas system. If a solid product layer forms between the gas and the reactive substrate, solid state diffusion fluxes will have to be included in the analysis, but the basis analysis logic is still the same.

ACKNOWLEDGEMENTS

The author wishes to acknowledge the U.S. National Science Foundation, Division of Materials Research, Grant No. DMR-8109260, for support of our CVD research, and his past and present graduate students for many stimulating discussions.

REFERENCES

1. M.M. Faktor and I. Garrett, Growth of Crystals from the Vapour, Chapman and Hall, London (1974).
2. D. Battat, M.M. Faktor, and I. Garrett, pp. 43-128 in Preparation and Properties of Solid State Materials, Vol. 2: Chemical Vapor Transport, Secondary Nucleation, and Mass Transfer in Crystal Growth (W.R. Wilcox, Ed.), Marcel Dekker, New York (1976).
3. D.W. Shaw, pp. 1-48 in Crystal Growth – Theory and Technique, Vol. 1 (C.H.L. Goodman, Ed.), Plenum Press, New York (1974).
4. M.E. Jones and D.W. Shaw, pp. 282-323 in Treatise on Solid State Chemistry, Vol. 5: Changes of State (N.B. Hannay, Ed.), Plenum Press, New York (1975).
5. C.H.J. van den Brekel, Philips Res. Repts. 32, 118-133 (1977).
6. J. Bloem, Pure & Appl. Chem. 50, 435-447 (1978).
7. G.M. Rosenblatt, pp. 165-240 in Treatise in Solid State Chemistry, Vol. 6A: Surfaces (N.B. Hannay, Ed.), Plenum Press, New York (1976).
8. G.M. Rosenblatt, J. Chem. Phys. 64, 3942-3950 (1976).
9. H. Schäfer, Chemical Transport Reactions, Academic Press, New York (1964).
10. K.E. Spear, pp. 1-16 in Reference 23.
11. C.B. Alcock and J.H.E. Jeffes, Trans. Instn. Min. Metall. (Sec. C) 76, C246-C258 (1967).
12. T.C. Wallace, Sr. and M.G. Bowman, Chemical Vapor Deposition: A Technique for Applying Protective Coatings, Los Alamos Scientific Lab. Rept. No. LA-UR 79-1470 (1979).
13. A.E. van Arkel and J.H. de Boer, Z. Anorg. Allgem. Chem. 148, 345 (1925).
14. R.F. Rolston, Iodide Metals and Metal Iodides, Wiley, New York (1961).
15. H. Schäfer, J. Crystal Growth 9, 17-30 (1971).
16. K. Fischer, private communication (1972).
17. Proceedings of the Conference on Chemical Vapor Deposition of Refractory Metals, Alloys, and Compounds (A.C. Schaffhauser, Ed.), American Nuclear Soc., Hinsdale, IL (1967).
18. Proceedings of the Second International Conference on Chemical Vapor Deposition (J.M. Blocher, Jr. and J.C. Withers, Eds.), The Electrochemical Soc., Princeton, NJ (1971).
19. Proceedings of the Third International Conference on Chemical Vapor Deposition (F.A. Glaski, Ed.), American Nuclear Soc., Hinsdale, IL (1972).
20. Proceedings of the Fourth International Conference on Chemical Vapor Deposition (G.F. Wakefield and J.M. Blocher, Jr., Eds.), The Electrochemical Soc., Princeton, NJ (1973).
21. Proceedings of the Fifth International Conference on Chemical Vapor Deposition (J.M. Blocher, Jr., H.E. Hinterman, and L.H. Hall, Eds.), The Electrochemical Soc., Princeton, NJ (1975).
22. Proceedings of the Sixth International Conference on Chemical Vapor Deposition (L.F. Donaghey, P. Rai-Choudhury, and R.N. Tauber, Eds.), The Electrochemical Soc., Princeton, NJ (1977).
23. Proceedings of the Seventh International Conference on Chemical Vapor Deposition (T.O. Sedgwick and H. Lydtin, Eds.), The Electrochemical Soc., Princeton, NJ (1979).
24. Proceedings of the Eighth International Conference on Chemical Vapor Deposition (J.M. Blocher, Jr., G.E. Vuillard, and G. Wahl, Eds.), The Electrochemical Soc., Princeton, NJ (1981).

25. R. Bonetti, Metal Progress (June), 44-47 (1981).
26. T.M. Besmann and K.E. Spear, J. Crystal Growth 31, 60-65 (1975).
27. T.M. Besmann and K.E. Spear, J. Electrochem. Soc. 124, 786-790 (1977).
28. T.M. Besmann and K.E. Spear, J. Electrochem. Soc. 124, 790-797 (1977).
29. L.R. Newkirk, R.E. Riley, H. Steinberg, F.A. Valencia, and T.C. Wallace, pp. 515-524 in Reference 23.
30. A.C. Cochran and J.B. Stephenson, Met. Trans. 1, 2875-2880 (1970).
31. K. Brennfleck, M. Dietrich, E. Fitzer, and D. Kehr, pp. 300-314 in Reference 23.
32. J.O. Carlsson, Chemical Vapour Deposition of Boron in a Closed System, Doctoral Thesis at Uppsala University, Sweden (1979).
33. Photograph was obtained in 1972 from the Metals and Ceramics Division, Oak Ridge National Laboratory, Oak Ridge, TN.
34. R.W. Kidd, M.F. Browning, and J.M. Rusin, pp. 563-577 in Reference 23.
35. L. Vandenbulcke, J. Electrochem. Soc. (in press), and to be published in Reference 24.
36. C. Bernard, to be published in Reference 24.
37. J.M. Blocher, Jr., J. Vac. Sci. Technol. 11, 680-686 (1974).
38. K.E. Spear and M.S. Wang, Solid State Techn. 23(7), 63-68 (1980).